

Study of hydroxyapatite doped with gadolinium and cerium ions using EPR spectroscopy methods

© M.A. Sadovnikova¹, G.V. Mamin¹, F.F. Murzakhanov¹, N.V. Petrakova², V.S. Komlev²,
M.R. Gafurov¹

¹ Institute of Physics, Kazan Federal University, Kazan, Russia

² Baikov Institute of Metallurgy and Materials Science, Russian Academy of Sciences, Moscow, Russia

E-mail: margaritaasadov@gmail.com

Received April 26, 2024

Revised June 12, 2024

Accepted October 30, 2024

Synthetic hydroxyapatites doped with rare earth ions (gadolinium and cerium) have been characterised using pulsed electron paramagnetic resonance methods. It was found that gadolinium and cerium ions are successfully incorporated into the hydroxyapatite crystal lattice, occupying the position of calcium ions (Ca²⁺).

Keywords: hydroxyapatite, electron paramagnetic resonance, rare earth elements.

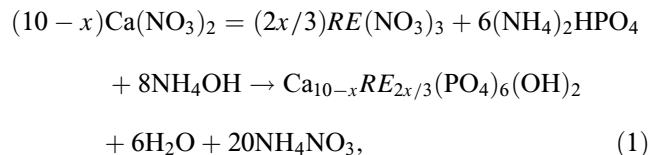
DOI: 10.61011/TPL.2024.12.60350.6410k

Biocompatible materials based on hydroxyapatite (HAP) with the Ca₁₀(PO₄)₆(OH)₂ chemical formula are currently used widely to restore bone tissue functions in clinical applications (specifically, in orthopedics, maxillofacial surgery, and implantology [1]). One important feature of HAP is that its structure allows for the inclusion of various impurity ions, which have the capacity to alter its biological and physicochemical properties even at low concentrations [2]. Rare earth elements (REEs), which are known for their role in production of phosphors, lasers, catalysts, several magnetic and superconducting materials, and contrast agents, have attracted particular attention in recent years as dopants for HAP [3,4]. While gadolinium (Gd³⁺) complexes are used to create contrast agents for magnetic resonance imaging [4], cerium (Ce) is of interest due to its transition valence of (III)→(IV), which has a positive effect on such properties of HAP as bacteriostatic action and antioxidant and antitumor activity [5]. In addition, luminescence induced by cerium ions provides an opportunity to produce fluorescent markers based on them [6]. Earlier studies have demonstrated that REEs are present in extremely low concentrations in the inorganic salt components of solid tissues of the human body, which play an important role in regulating the functions of cells and tissues [7]. Thus, the introduction of a certain amount of REEs into the crystal lattice of HAP may have a positive effect on the biomedical properties of this material and allow one to use the biomatrix for diagnostic imaging. In this context, the issues of analytical monitoring (qualitative and quantitative) of the introduction of REEs and other impurities into HAP become relevant.

Many important issues related to substitutions in HAP remain underexplored, and the data from various studies are contradictory. Since the choice of a suitable analytical method for detection of impurity structures is a debatable topic, the most significant discrepancies are found in data on the very feasibility of doping and the forms of incorporation

and localization of impurities in biominerals and synthetic samples. Traditional methods for examination of nanosized powders, ceramics, cements, coatings, and composites based on substituted HAP include X-ray diffraction analysis, infrared and Raman spectroscopy, scanning and transmission electron microscopy, etc. [8]. It has been demonstrated in our earlier studies that various electron paramagnetic resonance (EPR) methods, both standard and non-conventional for most analytical laboratories, may be used as an addition to the techniques indicated above not only for efficient detection and quantitative analysis of low concentrations of cationic and anionic paramagnetic impurities, but also for acquisition of unique data on the structural and magnetic properties of HAP doped with transition metal ions; the phase separation; phase transitions; types and magnitudes of spin-orbit, spin-lattice, and electron-nuclear interactions; etc. [9,10]. The present study is focused on characterization of synthetic HAP powders, which are doped with rare earth ions (Gd and Ce), by pulsed EPR.

Ce-containing (Ce-HAP) and Gd-containing (Gd-HAP) hydroxyapatites were synthesized by precipitation with the total molar ratio of calcium to phosphorus maintained at (Ca+REE)/P = 1.67 in accordance with the following reaction equation:

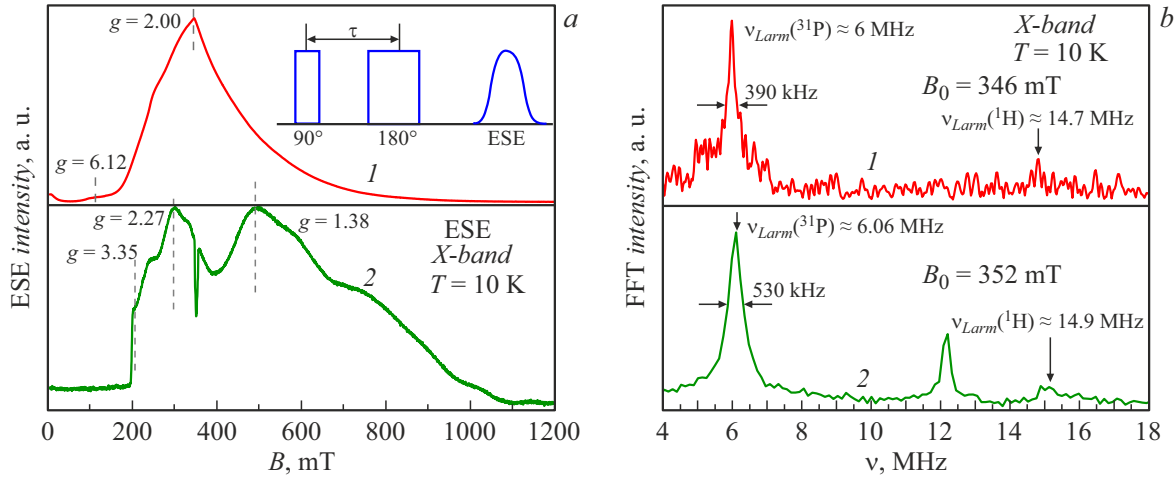


where RE stands for Gd or Ce, $x = ([\text{Ca}^{2+}]_y)/100$, and $y = 0.5\%$ for Ce and 0.25% for Gd [11].

The obtained suspensions were kept for 24 h in indoor conditions, filtered, and dried at 70°C for 48 h. Dried samples were ground to a fine powder and sieved through a 100 μm sieve. The synthesized powders were subjected to heat treatment in air at 1300°C.

Table 1. Relaxation times in the studied samples

Sample	$T_1, \mu\text{s}$	$T_2, \mu\text{s}$
Gd-HAP (10 K)	82 ± 3 ($B_0 = 346$ mT)	1.20 ± 0.05 ($B_0 = 346$ mT)
Ce-HAP (10 K)	127 ± 5 ($B_0 = 352$ mT)	2.4 ± 0.1 ($B_0 = 352$ mT)



a — Echo-detected EPR spectra of the dried Gd-HAP sample (1) and the Ce-HAP sample after heat treatment in air at 1300°C (2). These spectra were recorded using the Hahn pulse sequence; the $\pi/2$ pulse duration is 16 ns, and the interpulse time is $\tau = 240$ ns (the sequence is shown in the inset). *b* — Spectrum of nuclear transitions after Fourier transformation of the three-pulse ESEEM signal from Gd-HAP ($B_0 = 346$ mT) (1) and Ce-HAP ($B_0 = 352$ mT) (2) into the frequency domain.

EPR spectra were recorded at 10 K using an Elexsys E580 spectrometer (Bruker, Karlsruhe, Germany) at microwave frequency $\nu_{\text{MW}} = 9.6$ GHz (X band). Pulsed EPR spectra were obtained by measuring the integrated intensity of electron spin echo (ESE) in the Hahn sequence ($\pi/2 - \tau - \pi - \tau - \text{ESE}$), where the $\pi/2$ pulse duration is 16 ns. A similar sequence with time τ increasing in discrete steps at a fixed value of B was used to measure electron transverse relaxation time T_2 . An inversion–recovery sequence was used to measure longitudinal relaxation time T_1 . Electron–nuclear interactions manifested in the modulation of ESE decay and denoted in literature as ESEEM (electron spin echo envelope modulation) were analyzed with a three-pulse sequence ($\pi/2 - \tau - \pi/2 - T - \pi/2 - \tau - \text{ESE}$), where time parameter T was increased in discrete steps at a fixed value of $\tau = 240$ ns.

The observed resonant microwave absorption in the form of a broad line, which is presented in panel *a* of the figure (curve 1), corresponds to the EPR spectrum of the Gd-HAP sample. Gadolinium in ground state $^8S_{7/2}$ is paramagnetic and has electron spin $S = 7/2$ with zero orbital angular momentum $L = 0$. Disordered polycrystalline matrices doped with trivalent gadolinium ions were studied by EPR in [12,13]. Relying on the results reported in [12,13], we may state with certainty that the observed EPR resonance signal (curve 1 in panel *a* of the figure) corresponds to a Gd ion in the trivalent state ($g_{\text{eff}} = 6.12$ and $g = 2.00$).

Since a Ce^{3+} ion in the ground state has electron spin $S = 1/2$ and orbital angular momentum $L = 3$, EPR is suitable for detection of cerium ions in the trivalent state only. The presence of characteristic peaks in the EPR signal with g -factors equal to 3.35, 2.27, and 1.38 (curve 2 in panel *a* of the figure) suggests that the observed absorption line is induced by Ce^{3+} impurity centers [14]. The measured spin–lattice (T_1) and spin–spin (T_2) relaxation times for both REEs (Table 1) correspond to the relaxation times of REEs in several other crystals [15]. The relaxation times for gadolinium ions were found to be almost twice as short as those for cerium ions. One probable explanation of the shorter time T_2 for Gd^{3+} ions relative to the corresponding time for Ce^{3+} ions has to do (by analogy with a number of other transition metal ions; see [9]) with the fact that gadolinium ions may be localized at all calcium sites in the HAP lattice, while certain sites are more energetically favorable for cerium ions than others. Spin–spin interactions for the gadolinium ion sublattice are stronger in this case, shortening T_2 . It is reasonable to assume that time T_1 for a Gd^{3+} ion in HAP at low temperatures is short due to the greater efficiency of the single-phonon spin–lattice relaxation mechanism. However, in order to gain an insight into the mechanism of spin–lattice relaxation, one needs to analyze the temperature dependence of T_1 , which is planned to be carried out in future studies.

The presence of magnetic nuclei (^1H , nuclear spin $I = 1/2$; ^{31}P , $I = 1/2$) in the HAP structure induces a

Table 2. Distance between Ca^{2+} and ^{31}P determined via ESEEM peak analysis

Sample	B_0 , mT	r_{exp} , Å	r_{theory} , Å [16]
Gd-HAP	346	3.0 ± 0.4	3.2 (Ca1–P)
Ce-HAP	352	3.9 ± 0.3	3.4 (Ca2–P)

nuclear modulation envelope for the ESE decay curve, which makes it possible to obtain data on electron-nuclear interactions via Fourier transform of the three-pulse ESEEM time signal. The result for Gd-HAP is presented in panel *b* of the figure (curve 1). The peaks of phosphorus and, presumably, hydrogen nuclei at Larmor frequency $\nu_{Larm}(^{31}\text{P}) \approx 6$ MHz and $\nu_{Larm}(^1\text{H}) \approx 14.7$ MHz in fixed magnetic field $B_0 = 346$ mT provide evidence of successful introduction of the Gd^{3+} paramagnetic center into the HAP crystal lattice. The Ce-HAP spectra (curve 2 in panel *b* of the figure) feature ^{31}P ($\nu_{Larm}(^{31}\text{P}) \approx 6.06$ MHz) and ^1H ($\nu_{Larm}(^1\text{H}) \approx 14.9$ MHz) signals at $B_0 = 352$ mT. Thus, it was found that Ce ions are associated with phosphate groups and hydroxyl residues, and the presence of Ce in the HAP lattice was established.

Distance r from paramagnetic ions (Ce^{3+} and Gd^{3+}) to ^{31}P was calculated in the dipole-dipole approximation based on the line width at half maximum corresponding to the magnitude of unresolved anisotropic hyperfine interaction (A_{d-d}). The formula for calculation was as follows:

$$A_{d-d} \sim \frac{g_n g_e \mu_n \mu_e}{r^3},$$

where $g_n = 2.2632$ is the nuclear g -factor of ^{31}P and $g_e = 2.0023$ is the electron g -factor. The results are presented in Table 2.

A comparative analysis of the experimental estimate of distances and theoretical values (Table 2) verifies that REE ions occupy calcium sites.

Thus, the structural features of spin systems of powdered Gd-HAP and Ce-HAP were studied via pulsed EPR spectroscopy. The use of pulsed non-destructive EPR methods, which are highly sensitive to the presence of paramagnetic defects, made it possible to analyze electron-nuclear hyperfine interactions, identify nuclei near a paramagnetic ion, and estimate the distance between the nuclear and electron subsystems. A comprehensive study revealed the presence of gadolinium and cerium ions in the crystalline lattice of HAP. The obtained results demonstrate that EPR spectroscopy is an efficient experimental instrument for examining cationic REE doping.

Funding

This study was supported by grant No. 23-23-00640 from the Russian Science Foundation.

Conflict of interest

The authors declare that they have no conflict of interest.

References

- [1] Q.R.T. Lim, X.Y. Cheng, C.Y. Wee, *Adv. Mater. Sci. Technol.*, **5** (2) (2023). DOI: 10.37155/2717-526X-0502-1
- [2] A. Ressler, A. Žužić, I. Ivanišević, N. Kamboj, H. Ivanković, *Open. Ceram.*, **6**, 100122 (2021). DOI: 10.1016/j.oceram.2021.100122
- [3] V. Balaram, *Geosci. Front.*, **10** (4), 1285 (2019). DOI: 10.1016/j.gsf.2018.12.005
- [4] N. Iyad, M.S. Ahmad, S.G. Alkhatib, M. Hjouj, *Eur. J. Radiol. Open*, **11**, 100503 (2023). DOI: 10.1016/j.ejro.2023.100503
- [5] M.M. Farag, M.M. Ahmed, N.M. Abdallah, W. Swieszkowski, A.M. Shehabeldine, *Life Sci.*, **257**, 117999 (2020). DOI: 10.1016/j.lfs.2020.117999
- [6] J. Gao, L. Feng, B. Chen, B. Fu, M. Zhu, *Composites B*, **235**, 109758 (2022). DOI: 10.1016/j.compositesb.2022.109758
- [7] K. Saranya, S. Bhuvanewari, S. Chatterjee, N. Rajendran, *J. Mater. Sci.*, **55** (25), 11582 (2020). DOI: 10.1007/s10853-020-04742-z
- [8] M.A. Goldberg, O.S. Antonova, N.O. Donskaya, A.S. Fomin, F.F. Murzakhanov, M.R. Gafurov, A.A. Kononov, A.A. Kotyakov, A.V. Leonov, S.V. Smirnov, T.O. Obolkina, E.A. Kudryavtsev, S.M. Barinov, V.S. Komlev, *Nanomaterials*, **13**, 418 (2023). DOI: 10.3390/nano13030418
- [9] B. Gabbasov, M. Gafurov, A. Starshova, D. Shurtakova, F. Murzakhanov, G. Mamin, S. Orlinskii, *J. Magn. Magn. Mater.*, **470**, 109 (2019). DOI: 10.1016/j.jmmm.2018.02.039
- [10] F.F. Murzakhanov, G.V. Mamin, M.A. Goldberg, A.V. Knotko, M.R. Gafurov, S.B. Orlinskii, *Russ. J. Coord. Chem.*, **46**, 729 (2020). DOI: 10.1134/S1070328420110044
- [11] A.Yu. Demina, N.V. Petrakova, F.F. Murzakhanov, G.V. Mamin, Yu.O. Nikitina, M.A. Sadovnikova, S.O. Andreev, A.V. Zhukov, M.R. Gafurov, V.S. Komlev, *Magn. Reson. Solids*, **25** (3), 23303 (2023). DOI: 10.26907/mrsej-23303
- [12] V. Singh, C.B. Annapurna Devi, B.R.V. Rao, A.S. Rao, N. Singh, B.M. Mistry, *Optik*, **226**, 165932 (2021). DOI: 10.1016/j.ijleo.2020.165932
- [13] M.A. Sadovnikova, F.F. Murzakhanov, I.V. Fadeeva, A.A. Forsyenkova, D.V. Deyneko, G.V. Mamin, M.R. Gafurov, *Ceramics*, **5** (4), 1154 (2022). DOI: 10.3390/ceramics5040081
- [14] N.V. Petrakova, Y.O. Zobkova, V.S. Komlev, A.A. Ashmarin, A.S. Lysenkov, V.A. Volchenkova, S.M. Barinov, M.A. Sadovnikova, F.F. Murzakhanov, M.R. Gafurov, E.A. Kudryavtsev, S.A. Kozyukhin, A.L. Trigub, A.V. Rogachev, *Ceram. Int.*, **50** (12), 20905 (2024). DOI: 10.1016/j.ceramint.2024.03.093
- [15] *Multifrequency electron paramagnetic resonance*, ed. by S.K. Misra (John Wiley & Sons, Ltd., U.K., 2011).
- [16] Y. Tang, H.F. Chappell, M.T. Dove, R.J. Reeder, Y.J. Lee, *Biomaterials*, **30** (15), 2864 (2009). DOI: 10.1016/j.biomaterials.2009.01.043

Translated by D.Safin